



Enhanced visible-light-induced photocatalytic activity of $\alpha\text{-Fe}_2\text{O}_3$ adsorbing redox enzymes



Kai Kamada^{a,*}, Nobuaki Soh^b

^a Department of Materials Science and Engineering, Faculty of Engineering, Nagasaki University, Nagasaki 852-8521, Japan

^b Faculty of Agriculture, Saga University, Saga 840-8502, Japan

ARTICLE INFO

Article history:

Received 18 June 2014

Received in revised form 9 October 2014

Accepted 13 October 2014

Available online 2 November 2014

Keywords:

Redox enzyme

Photocatalyst

Bio-inorganic hybrid

ABSTRACT

We report fabrication of hybrid photocatalyst composed of an n-type semiconductor ($\alpha\text{-Fe}_2\text{O}_3$) and a redox enzyme (horseradish peroxidase; HRP), and its performance for oxidation of luminol in an aqueous solution. The hybrid photocatalyst is simply formed via physical adsorption of HRP to an $\alpha\text{-Fe}_2\text{O}_3$ sintered body. Under visible light irradiation, the bare $\alpha\text{-Fe}_2\text{O}_3$ with a narrow bandgap photocatalytically oxidizes luminol along with blue emission that can be used as an indicator of the photocatalytic performance. The blue emission is largely strengthened after the adsorption of HRP, demonstrating that the presence of enzyme improves apparent photocatalytic activity of $\alpha\text{-Fe}_2\text{O}_3$. The favorable effect is derived from synergistic oxidation of luminol by the biocatalysts (HRP) as well as by the photocatalyst ($\alpha\text{-Fe}_2\text{O}_3$). In this paper, influence of excitation wavelength, adsorption amount of HRP, and reaction temperature on the overall photocatalytic activity are elucidated, and then a reaction mechanism of the proposed novel hybrid photocatalyst is discussed in detail.

© 2014 The Ceramic Society of Japan and the Korean Ceramic Society. Production and hosting by Elsevier B.V. All rights reserved.

1. Introduction

$\alpha\text{-Fe}_2\text{O}_3$ (hematite) is abundant in nature and a thermodynamically stable n-type semiconductor, and thus is widely applied for various applications such as batteries [1], sensors [2], pigments [3], etc. In addition, due to the relatively narrow bandgap (2.2 eV), $\alpha\text{-Fe}_2\text{O}_3$ is utilized as a photocatalyst or an electrode of photoelectrochemical cell for energy resource production and purification of pollutants that work under visible light irradiation [4–8]. However, $\alpha\text{-Fe}_2\text{O}_3$ harvests only 40% of sunlight because of the narrow bandgap, and electron-hole pairs produced by irradiation are readily recombined thanks to a short diffusion length of hole in addition to a low electrical conductivity [9]. In recent years, these drawbacks have been solved through various strategies. For instance, formation of micro-/nano-structures broadens a surface area exposed to a light source and reactants [10–14]. Introduction of aliovalent dopants into the crystal lattice increases carrier density and hence raises the electrical conductivity [15–18]. Hybridization with other materials diminishes the charge recombination [19,20]. Li et al. have claimed that hybridizing of $\alpha\text{-Fe}_2\text{O}_3$ with another semiconductor (Bi_2O_3) extends a range of absorption

wavelength and promotes charge separation due to a difference in band edge position [21]. Thomann et al. have shown that loading of Au nanoparticles is useful for enhancing the photoabsorption efficiency due to a surface plasmon excitation of the nanoparticles [22]. Needless to say, on the other hand, addition of sacrificial electron acceptor or donor promotes photocatalytic reaction [23].

Needless to say, semiconductor photocatalysts contribute oxidation/reduction (redox reaction) because both electrons in conduction band (CB) and holes in valence band (VB) participate in the reaction. On the other hand, enzymes are recognized as biocatalysts with an excellent catalytic activity even in moderate conditions. One can use enzymes as environmentally benign catalysts since their protein framework contains few heavy metals. Therefore, in vitro utilization of enzymes is frequently performed especially in the fields of chemical or food/beverage industries. Enzymes are classified according to a reaction they catalyze or initiate (hydrolysis, dehydration, isomerization, etc.). Among them, redox enzymes stimulate an oxidation/reduction of substrate as similar to photocatalysts. Therefore, in order to enhance the photocatalytic activity of $\alpha\text{-Fe}_2\text{O}_3$ under visible light irradiation, a novel hybrid photocatalyst composed of the $\alpha\text{-Fe}_2\text{O}_3$ and the redox enzyme is proposed in the present study. A schematic reaction model of the hybrid photocatalyst is illustrated in Fig. 1, where luminol (L) is employed as a reactant. The $\alpha\text{-Fe}_2\text{O}_3$ itself acts as a photocatalyst under irradiation of visible light (Fig. 1a), and then chemiluminescence (CL) is observed as a result of photocatalytic oxidation of luminol, whereas, in the case of hybrid

* Corresponding author. Tel.: +81 95 819 2667; fax: +81 95 819 2667.

E-mail address: kkamada@nagasaki-u.ac.jp (K. Kamada).

Peer review under responsibility of The Ceramic Society of Japan and the Korean Ceramic Society.

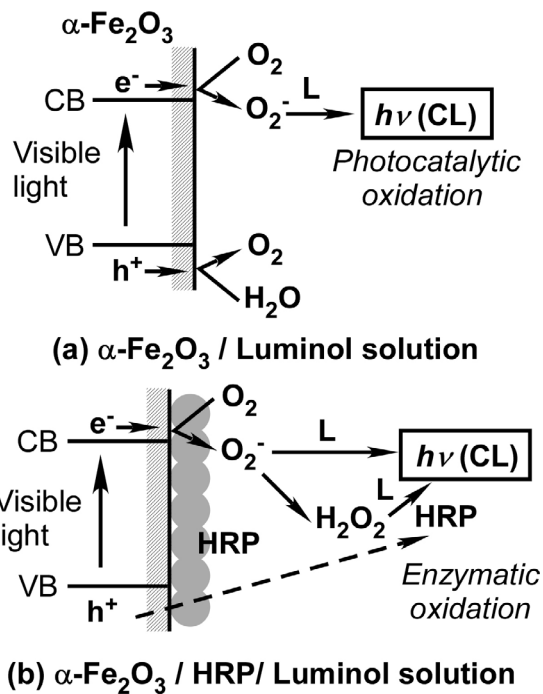


Fig. 1. Schematic model of visible-light-induced photocatalytic oxidation of luminol (L) accompanied by chemiluminescence (CL) on (a) bare $\alpha\text{-Fe}_2\text{O}_3$ and (b) HRP-adsorbed $\alpha\text{-Fe}_2\text{O}_3$.

photocatalysts (Fig. 1b), redox enzyme (horseradish peroxidase, HRP) is adsorbed on surface of $\alpha\text{-Fe}_2\text{O}_3$ via an electrostatic interaction, and then photogenerated species (H_2O_2 and/or hole) trigger an enzymatic oxidation of luminol. That is, the photocatalytic and the photo-induced enzymatic oxidation for an identical reactant occur simultaneously, resulting in enhancement of apparent reaction rate. From the other perspective, it should be noted that the proposed technique accomplishes photochemical activity control of enzymes frequently described in the recent literatures [24–27].

It is familiar that enzymes possess excellent substrate specificity and reaction selectivity. In contrast, reaction possibility of a semiconductor photocatalyst is determined only by a relationship between a band edge position and a redox potential of reactant (substrate), leading to poor substrate specificity and reaction efficiency. The hybrid photocatalysis proposed here may overcome the non-specific reaction on semiconductor and yield only desired product without any side reactions. Furthermore, the hybridization with inorganic semiconductors would be effective for stabilizing enzymes having poor physicochemical durability as similar to conventional immobilized enzymes. In this study, HRP is adsorbed on surface of $\alpha\text{-Fe}_2\text{O}_3$ sintered body, and then influence of the HRP adsorption on the photocatalytic activity for the luminol oxidation is investigated under visible light irradiation, because luminol is oxidized both by semiconductor photocatalysts and HRP. Consequently, it is demonstrated that the existence of HRP on $\alpha\text{-Fe}_2\text{O}_3$ surface effectively increases the oxidation activity. Within our knowledge, it is the first report that the hybridization of $\alpha\text{-Fe}_2\text{O}_3$ with redox enzymes causes the enhanced photocatalytic activity under visible light irradiation.

2. Experimental

$\alpha\text{-Fe}_2\text{O}_3$ and horseradish peroxidase (HRP, MW 42,000) were employed as a semiconductor photocatalyst and a redox enzyme, respectively. Commercially available $\alpha\text{-Fe}_2\text{O}_3$ microcrystalline powder (2.0 g) was mixed with an aqueous solution of polyvinyl

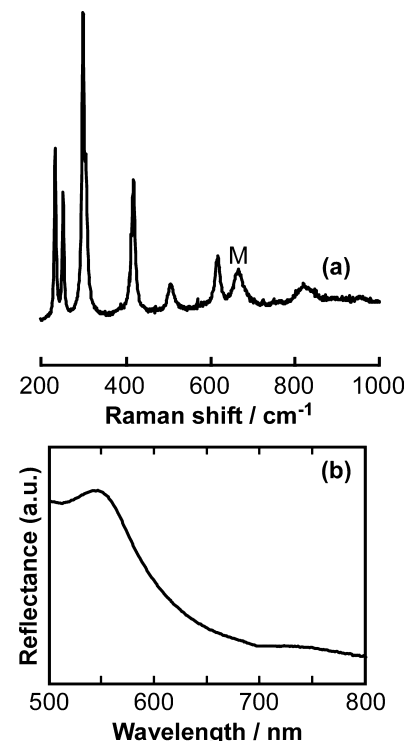


Fig. 2. (a) Raman and (b) UV-vis diffuse-reflectance spectra of $\alpha\text{-Fe}_2\text{O}_3$ polycrystal sintered at 1250 °C for 3 h. The peak M in (a) indicates presence of magnetite (Fe_3O_4) and all other peaks are assigned to hematite phase.

alcohol (PVA, 0.1 g/mL, 1 mL) as a binder followed by drying at 100 °C. The resultant powder was pressed uniaxially and then was sintered at 1350 °C for 3 h in air to obtain an $\alpha\text{-Fe}_2\text{O}_3$ pellet (diameter = 6.4 mm, thickness = 0.5 mm). A scanning electron microscopy (SEM) was utilized to observe morphology of the pellet. Crystal structure and optical absorption property were characterized by a Raman and a UV-vis diffuse reflectance spectroscopies, respectively. To adsorb HRP molecules, the pellet was immersed in a solution dissolving HRP (0.1–1.8 mg/mL in 5 mM citrate buffer solution at pH = 6.5) at room temperature. The HRP-adsorbed $\alpha\text{-Fe}_2\text{O}_3$ (denoted below as HRP- $\alpha\text{-Fe}_2\text{O}_3$) was immersed in deionized water for several seconds to remove unbound HRP molecules. Photocatalytic activity of HRP- $\alpha\text{-Fe}_2\text{O}_3$ was evaluated for oxidation of luminol as a model reaction. The HRP- $\alpha\text{-Fe}_2\text{O}_3$ was set to a flat well bottom of black microplate (96-well), and then 0.338 mM luminol solution (150 μ L, buffered at pH = 9 with 0.1 M Tris-HCl) was injected to the well. To initiate the photocatalytic reaction, the well was exposed to visible light with three classes of wavelength (monochromated by band pass filters: peak wavelength/fwhm: 645/40, 590/20, and 530/25 nm) at a certain temperature. Intensity of chemiluminescence through a band pass filter of 460/40 nm originated from the luminol oxidation was recorded as a relative luminescence unit (RLU) for 20 ms on a microplate reader. The identical measurement was repeated four times at least to secure reliable results. A 1 wt% Pt-loaded $\alpha\text{-Fe}_2\text{O}_3$ pellets was also fabricated and employed for the photocatalytic reaction. In this case, the $\alpha\text{-Fe}_2\text{O}_3$ powder dispersed in an aqueous solution of H_2PtCl_6 was dried at 70 °C and then sintered at the identical condition.

3. Results and discussion

The sintering of $\alpha\text{-Fe}_2\text{O}_3$ powder induced formation of a dense polycrystal with relative density of more than 90% (Supplementary data, Fig. 1S). According to the Raman spectrum in Fig. 2a, the pellet was mainly composed of hematite ($\alpha\text{-Fe}_2\text{O}_3$) phase containing a

trace amount of magnetite (Fe_3O_4 , labeled as M in the spectrum), which has been frequently detected in $\alpha\text{-Fe}_2\text{O}_3$ nanomaterials by Raman spectroscopy [16]. Fig. 2b shows the UV-vis diffuse-reflectance spectrum of the $\alpha\text{-Fe}_2\text{O}_3$ pellet. The $\alpha\text{-Fe}_2\text{O}_3$ absorbed visible light over a wide wavelength range. The absorption edge was observed at ca. 630 nm, suggesting a contribution of indirect transition (Fe^{3+} 3d → 3d) [13,14]. These facts support that visible light with a shorter wavelength than 630 nm has sufficient energy to excite the $\alpha\text{-Fe}_2\text{O}_3$.

The adsorption of HRP to the $\alpha\text{-Fe}_2\text{O}_3$ surface was conducted by immersion in the HRP solution at pH 6.5. Taking into account isoelectric point of HRP ($pI \sim 5$) [28] and $\alpha\text{-Fe}_2\text{O}_3$ ($pI \sim 9$) [29], the HRP charges negatively at pH 6.5 in contrast that the $\alpha\text{-Fe}_2\text{O}_3$ has an opposite surface charge. Hence, it seems that the HRP can be fixed on the $\alpha\text{-Fe}_2\text{O}_3$ surface through electrostatic interaction between them. In fact, the weak absorption bands assigned to amide I (1650 cm^{-1}) and II (1540 cm^{-1}) of protein framework were observed in the FT-IR spectrum of $\alpha\text{-Fe}_2\text{O}_3$ after the adsorption (Fig. 2S) [30]. Consequently, it was revealed that the immobilization of HRP to the $\alpha\text{-Fe}_2\text{O}_3$ surface was successfully achieved via the simple electrostatic interaction.

Several previous papers have described that n-type semiconductors, especially TiO_2 gives rise to photocatalytic oxidation of luminol accompanied by chemiluminescence under UV light irradiation [31–34]. In an alkaline aqueous solution, electrons excited to the conduction band (CB) of TiO_2 reduce dissolved oxygen molecules, resulting in generation of superoxide anion radicals ($\bullet\text{O}_2^-$). On the other hand, holes produced in the valence band (VB) oxidize hydroxide ions (OH^-) to hydroxyl radicals ($\bullet\text{OH}$). Luminol is attacked by both the radicals, and then is converted into a 3-aminophtharic acid with a blue emission (Fig. 3S). Visible light irradiation to the bare $\alpha\text{-Fe}_2\text{O}_3$ would trigger the chemiluminescence of luminol via an analogous process (Fig. 1a). Based on the energy level diagram reported in the literature [35], the CB and the VB edges of polycrystalline $\alpha\text{-Fe}_2\text{O}_3$ have been estimated to be located at ca. -0.6 and $+1.6\text{ V}$ vs. standard hydrogen electrode (SHE) at pH 9, respectively. That is, photogenerated electrons can reduce dissolved oxygen molecules ($\text{O}_2/\bullet\text{O}_2^-$, $E^\circ = -0.28\text{ V}$), while the oxidation of OH^- by holes seems to be thermodynamically impossible ($\text{OH}^-/\bullet\text{OH}$, $E^\circ = +1.85\text{ V}$) [36,37]. Instead, the holes should be consumed by oxidation of OH^- to O_2 ($E^\circ = +0.70\text{ V}$). Hence, the photocatalytic oxidation of luminol on the irradiated $\alpha\text{-Fe}_2\text{O}_3$ is anticipated to be caused by the $\bullet\text{O}_2^-$. Xu et al. have claimed that generation of reactive oxygen species including radicals in $\alpha\text{-Fe}_2\text{O}_3$ aqueous suspension is originated from O_2 -reduction by photogenerated electrons rather than oxidation by holes because the process was inhibited under anaerobic conditions [38]. In the present study, we detected the $\bullet\text{O}_2^-$ under the visible light irradiation to bare $\alpha\text{-Fe}_2\text{O}_3$ by means of the reduction assay of cytochrome c (Fig. 4S).

Fig. 3 includes the relative luminescence unit (RLU) of 0.338 mM luminol on the bare $\alpha\text{-Fe}_2\text{O}_3$ (open columns), which was integrated for the period of exposure to the visible lights with different wavelength ranges. The RLU was measured through a band pass filter (460/40 nm) to eliminate diffuse-reflections of the excitation light. As expected, no chemiluminescence was observed under the excitation light with lower photon energy than the absorption edge of $\alpha\text{-Fe}_2\text{O}_3$ (645/40 nm). On the other hand, the visible lights possessing high photon energy (590/35 and 530/25 nm) successfully caused the blue emission. Since the maximum emission intensity of luminol was observed at ca. 433 nm at pH 9 (Fig. 3S), the resultant chemiluminescence might also contribute to the bandgap excitation of $\alpha\text{-Fe}_2\text{O}_3$. These facts indicate that the luminol can be photocatalytically oxidized under the presence of $\alpha\text{-Fe}_2\text{O}_3$ exposed to visible light.

Fig. 3 includes the RLU measured under the existence of HRP- $\alpha\text{-Fe}_2\text{O}_3$ (closed columns), where the 0.8 mg/mL HRP solution was

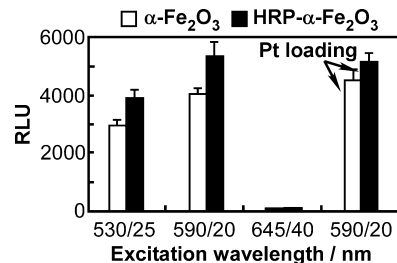


Fig. 3. Effect of HRP adsorption on relative luminescence unit (RLU, 460/40 nm) of 0.338 mM luminol under the presence of $\alpha\text{-Fe}_2\text{O}_3$ exposed to three classes of visible lights (530/25, 590/20, and 645/40 nm) for 20 ms at pH 9. The open and closed columns correspond to RLU of bare $\alpha\text{-Fe}_2\text{O}_3$ and HRP- $\alpha\text{-Fe}_2\text{O}_3$, respectively. The data obtained using 1 wt% Pt-loaded $\alpha\text{-Fe}_2\text{O}_3$ are also displayed. The error bars indicate standard deviations.

employed for the adsorption procedure. As shown in Fig. 3, the RLU of luminol solution was largely increased as a result of the HRP adsorption on the $\alpha\text{-Fe}_2\text{O}_3$ surface. That is, the apparent photocatalytic activity of $\alpha\text{-Fe}_2\text{O}_3$ was improved under the presence of HRP. Since a tungsten-halogen lamp, which had a maximum intensity at $\lambda = 1000\text{ nm}$, was employed for excitation, the RLUs at 590/20 nm were larger than those at 530/25 nm with higher photon energy. The enhanced activity can be explained as follows (Fig. 1b). In general, HRP requires peroxides such as H_2O_2 and ROOH in order to oxidize electron donors like luminol. Under the illumination, the $\bullet\text{O}_2^-$ produced at the $\alpha\text{-Fe}_2\text{O}_3$ surface is transformed into H_2O_2 through spontaneous disproportionation, and then the resting HRP (reduced state) is activated to excited (oxidized) state by the H_2O_2 . Also, the holes in the VB may directly activate the HRP [39]. Subsequently, the excited HRP leads to enzymatic oxidation of luminol accompanied by two-electron reduction to regenerate the resting state. Consequently, the observed RLU enhancement is considered to be based on the enzymatic oxidation of luminol. In fact, our previous paper has confirmed that HRP intercalated into titanate nanosheets with a wide bandgap can be excited by UV light irradiation without an addition of peroxides [40]. When 1 wt% Pt-loaded $\alpha\text{-Fe}_2\text{O}_3$ was utilized (rightmost columns in Fig. 3), the RLU enhancement (15%) was lesser than that when the pure $\alpha\text{-Fe}_2\text{O}_3$ was used (ca. 33%). Since the Pt-loading stimulated charge separation efficiency of the irradiated $\alpha\text{-Fe}_2\text{O}_3$ [20], the photocatalytic performance could be improved without the immobilization of HRP. As a result, we have firstly demonstrated in the present study that the photocatalytic reaction of luminol on the $\alpha\text{-Fe}_2\text{O}_3$ was promoted by the hybridization with HRP.

Fig. 4a displays the influence of adsorption amount of HRP on the luminol oxidation. Since an adsorption amount of HRP was too small to be estimated, the horizontal axis is expressed as the concentration of HRP solution used for the adsorption that should be concerned with an actual amount existing on the $\alpha\text{-Fe}_2\text{O}_3$ surface. On the other hand, the vertical axis means the percentage of RLU enhancement by the HRP adsorption. The figure revealed that the RLU enhancement tended to rise with increasing the adsorption amount at the low concentration range of HRP. The fact again supports the photocatalytic reaction of luminol boosted by the enzymatic oxidation. However, the enhancement reached a maximum at 1.0 mg/mL, and then was reduced as the concentration was further increased, and finally became negative at 1.8 mg/mL. In our previous paper [39], the saturated adsorption amount of HRP on an $\alpha\text{-Fe}_2\text{O}_3$ thin film with relatively flat surface was estimated to be 2.9 $\mu\text{g}/\text{cm}^2$. Assuming that HRP molecules were densely adsorbed on a solid surface, a thickness of surface HRP layer was calculated to be ca. 26 nm (4.4 molecules). This means that such multilayer adsorption of HRP would disturb access of O_2 and H_2O to the $\alpha\text{-Fe}_2\text{O}_3$ especially at high HRP concentrations over 1.0 mg/mL.

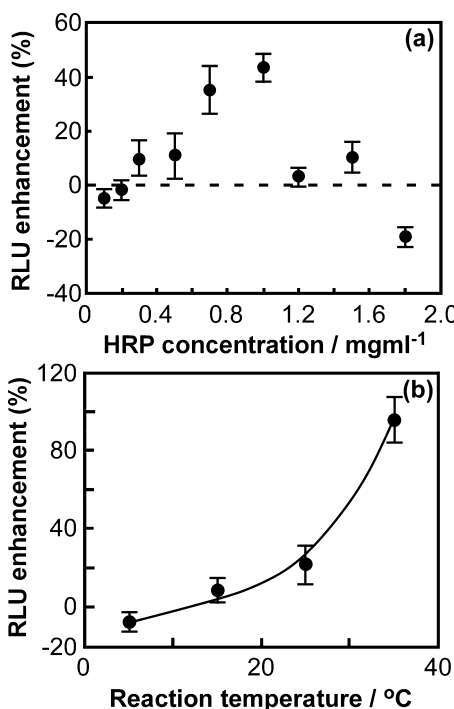


Fig. 4. Influence of (a) adsorption amount of HRP and (b) reaction temperature on HRP-assisted photocatalytic oxidation of luminol. The vertical axes are described as the percentage of RLU enhancement by HRP adsorption. The error bars indicate standard deviations.

Moreover, the visible light absorption of the $\alpha\text{-Fe}_2\text{O}_3$ might be also retarded by the existence of brownish HRP. Therefore, it has been revealed that an optimum HRP absorption amount is present for the visible-light-driven luminol oxidation using the HRP- $\alpha\text{-Fe}_2\text{O}_3$. Fig. 4b shows the dependence of reaction temperature on the RLU enhancement, where 1.0 mg/mL HRP was employed for the adsorption. The favorable effect of HRP adsorption was prominent especially at high temperature and the RLU enhancement reached ca. 100% (two times) at 35 $^{\circ}\text{C}$. Since the optimum working temperature of HRP is reported to be about 45 $^{\circ}\text{C}$ independent of whether HRP is immobilized on a support or not [41], high reaction temperature appears to be preferred to accelerate the photocatalytic oxidation of luminol assisted by the HRP.

4. Conclusions

The present study investigated the visible-light-induced photocatalytic performance of $\alpha\text{-Fe}_2\text{O}_3$ hybridized with the redox enzyme (HRP). Under visible light illumination, bare $\alpha\text{-Fe}_2\text{O}_3$ showed a certain photocatalytic oxidation activity for luminol. In this process, dissolved O_2 molecules were transformed into $\cdot\text{O}_2^-$ by photogenerated electrons in the conduction band of irradiated $\alpha\text{-Fe}_2\text{O}_3$, and then the radicals reacted with the luminol. HRP was easily immobilized on $\alpha\text{-Fe}_2\text{O}_3$ surface via an electrostatic interaction. It was confirmed that the overall oxidation activity was increased after the immobilization of HRP, because the adsorbed HRP also induced the enzymatic oxidation of luminol under the presence of H_2O_2 that was formed by disproportionation of $\cdot\text{O}_2^-$. The HRP might be also activated by direct hole transfer from the valence band of $\alpha\text{-Fe}_2\text{O}_3$ exposed to colored light. Since enzyme generally contributes a specific reaction and there are a variety of redox enzymes that catalyze diverse chemical reactions, the present hybridization technique would be useful for improving a reaction/reactant selectivity of semiconductor photocatalysts.

Acknowledgments

The present work was partly supported by Grant-in-Aid for Young Scientists (Nos. 24750205 and 24750072) from Japan Society for the Promotion of Science (JSPS).

Appendix A. Supplementary data

Supplementary data associated with this article can be found, in the online version, at doi:10.1016/j.jascer.2014.10.004.

References

- [1] K. Brezesinski, J. Haetge, J. Wang, S. Mascotto, C. Reitz, A. Rein, S.H. Tolbert, J. Perlich, B. Dunn and T. Brezesinski, *Small*, **7**, 407–414 (2011).
- [2] J. Chen, L. Xu, W. Li and X. Gou, *Adv. Mater.*, **17**, 582–586 (2005).
- [3] A.L. Costa, F. Matteucci, M. Dondi, I. Zama, S. Albonetti and G. Baldi, *J. Eur. Ceram. Soc.*, **28**, 169–176 (2008).
- [4] W. Sun, Q. Meng, L. Jing, D. Liu and Y. Cao, *J. Phys. Chem. C*, **117**, 1358–1365 (2013).
- [5] M.M. Khader, G.H. Vurens, I.-K. Kim, M. Saleron and G.A. Somorjai, *J. Am. Chem. Soc.*, **109**, 3581–3585 (1987).
- [6] T. Kawahara, K. Yamada and H. Tada, *J. Colloid Interface Sci.*, **294**, 504–510 (2006).
- [7] V.R. Satsangi, S. Kumari, A.P. Singh, R. Shrivastav and S. Dass, *Int. J. Hydrogen Energ.*, **33**, 312–318 (2008).
- [8] A. Ansari, J. Peral, X. Doménech and R. Rodríguez-Clemente, *Environ. Pollut.*, **95**, 283–288 (1997).
- [9] N. Beermann, L. Vayssières, S.-E. Lindquist and A. Hagfeldt, *J. Electrochem. Soc.*, **147**, 2456–2461 (2000).
- [10] K.P. Gajendra and K.M. Parida, *ACS Appl. Mater. Interfaces*, **3**, 317–323 (2011).
- [11] J. Qu, Y. Yu, C.-Y. Cao and W.-G. Song, *Chem. Eur. J.*, **19**, 11172–11177 (2013).
- [12] W. Wu, R. Hao, F. Liu, X. Su and Y. Hou, *J. Mater. Chem. A*, **1**, 6888–6894 (2013).
- [13] A. Kay and M. Grätzel, *J. Am. Chem. Soc.*, **128**, 15714–15721 (2006).
- [14] A. Duret and M. Grätzel, *J. Phys. Chem. B*, **109**, 17184–17191 (2005).
- [15] J.S. Jang, K.Y. Yoon, X. Xiao, F.-R. Fan and A.J. Bard, *Chem. Mater.*, **21**, 4803–4810 (2009).
- [16] Y.-S. Hu, A. Kleinman-Shwarsstein, A.J. Forman, D. Hazen, J.-N. Park and E.W. McFarland, *Chem. Mater.*, **20**, 3803–3805 (2008).
- [17] P. Liao, M.C. Toroker and E.A. Carter, *Nano Lett.*, **11**, 1775–1781 (2011).
- [18] J.A. Glasscock, P.R.F. Barnes, I.C. Plumb and N. Savvides, *J. Phys. Chem. C*, **111**, 16477–16488 (2007).
- [19] S. Bai, S. Shuangjiang, Z. Xiaoping and G. Wang, *RSC Adv.*, **2**, 10977–10984 (2012).
- [20] Z. Zhang, F. Md, T. Hossain, T. Miyazaki and Takahashi, *Environ. Sci. Technol.*, **44**, 4741–4746 (2010).
- [21] J. Li, J. Zhong, X. He, S. Huang, J. Zeng, J. He and W. Shi, *Appl. Surf. Sci.*, **284**, 527–532 (2013).
- [22] I. Thomann, B.A. Pinaud, Z. Chen, B.M. Clemens, T.F. Jaramillo and M.L. Brongersma, *Nano Lett.*, **11**, 3440–3446 (2011).
- [23] O. Akhavan and R. Azimirad, *Appl. Catal. A*, **369**, 77–82 (2009).
- [24] S. Kohse, A. Neubauer, A. Pazidis, S. Lochbrunner and U. Kragl, *J. Am. Chem. Soc.*, **135**, 9407–9411 (2013).
- [25] L. Fruk, V. Rajendran, M. Spengler and M. Niemeyer, *ChemBioChem*, **8**, 2195–2198 (2007).
- [26] J.C. Bretschneider, M. Reismann, M.G. Plessen and U. Simon, *Small*, **5**, 2549–2553 (2009).
- [27] F. Kurayama, T. Matsuyama and H. Yamamoto, *Adv. Powder. Technol.*, **15**, 51–61 (2004).
- [28] K. Kamada, S. Tsukahara and N. Soh, *J. Mater. Chem.*, **20**, 5646–5650 (2011).
- [29] M. Oćwieja, Z. Adamczyk, M. Morga, E. Bielańska and A. Węgrzynowicz, *J. Colloid Interface Sci.*, **386**, 51–59 (2012).
- [30] C.V. Kumar and A. Chaudhari, *J. Am. Chem. Soc.*, **122**, 830–837 (2000).
- [31] T. Hirakawa, H. Kominami, B. Ohtani and Y. Nosaka, *J. Phys. Chem. B*, **105**, 6993–6999 (2001).
- [32] K. Ishibashi, A. Fujishima, T. Watanabe and K. Hashimoto, *J. Phys. Chem. B*, **104**, 4934–4938 (2000).
- [33] H. Xu, H. Ye, X. Zhu, S. Liang, L. Guo, Z. Lin, X. Liu and G. Chen, *Analyst*, **138**, 234–239 (2013).
- [34] T. Daimon, T. Hirakawa, M. Kitazawa, J. Suetake and Y. Nosaka, *Appl. Catal. A-Gen.*, **340**, 169–175 (2008).
- [35] J.J. Kennedy and K.W. Frese Jr., *J. Electrochem. Soc.*, **125**, 723–726 (1978).
- [36] J.P. Hoare, in *Standard Potentials in Aqueous Solution*, Ed. by A.J. Bard, R. Parsons and J. Jordan, CRC Press, New York (1995) pp. 61–62.
- [37] G.K. Pradhan, N. Sahu and K.M. Parida, *RSC Adv.*, **3**, 7912–7920 (2013).
- [38] J. Xu, N. Sahai, C.M. Eggleston and M.A.A. Schoonen, *Earth Planet. Sci. Lett.*, **363**, 156–167 (2013).
- [39] K. Kamada, A. Moriyasu and N. Soh, *J. Phys. Chem. C*, **116**, 20694–20699 (2012).
- [40] K. Kamada, T. Nakamura and S. Tsukahara, *Chem. Mater.*, **23**, 2968–2972 (2011).
- [41] M. Monier, D.M. Ayad, Y. Wei and A.A. Sarhan, *Int. J. Biol. Macromol.*, **46**, 324–330 (2010).